Journal of Chemical and Petroleum Engineering (JChPE)

Print ISSN: 2423-673X Online ISSN: 2423-6721

Influence of Nozzle Numbers on Analysis of Air- Water Flow in a Rotating Packed Bed with Computational Fluid Dynamics

Shamsedin Ghourejili, Ali Reza Miroliaei *

1. Department of Chemical Engineering, University of Mohaghegh Ardabili, Ardabil, Iran. E-mail: ghourejili.sh@wefinder.ir
2. Department of Chemical Engineering, University of Mohaghegh Ardabili, Ardabil, Iran. E-mail: armiroliaei@uma.ac.ir

ARTICLE INFO

Article History:
Received: 27 January 2023
Revised: 21 August 2023
Accepted: 17 September 2023

Article type: Research

Keywords:
RPB,
CFD,
Analysis of Air-Water,
Flooding,
Uniform Flow Pattern

ABSTRACT

Nowadays, rotating packed beds (RPBs) have been adopted in the many chemical processes such as absorption, desorption, distillation, and etc. Due to the complex structure of RPBs, Computational Fluid Dynamic (CFD) is adopted for analyzing air-water flow in the RPB. In this work, increasing nozzle from 2 to 8 on the behavior of air and water flows was investigated and validated with the experimental data with deviations less than 14%. The obtained results of RPB with packing and baffles demonstrated that increasing nozzle from 2 to 6 increased air velocity vectors. Also, increasing nozzle from 2 to 6 in the RPB with packing uniformed the water velocity on the rotor and housing. In the end, RPB with baffles increased momentum of water velocity vectors and velocity gradient on the rotor and housing. The obtained results showed that the RPB with 6 nozzles have the uniform air flow pattern rather than other nozzle design. Also, in the RPB with baffles; flooding occurred in all sections of the RPB with 8 nozzles. Furthermore, velocity vectors of the outer edge rotor were larger than the inner edge rotor in the RPB with packing and baffles.

Introduction

Nowadays, RPB known as high-gravity devices have been extensively paid attention by chemical engineering. RPBs have lower volume and less operating cost than the conventional packed beds [1-7]. RPBs was invented by Ramshaw and Malinsow in 1981 [8]. RPBs can exploit centrifugal force up to several hundred times greater than the gravitational force. So, under the high centrifugal field of the RPB, the thin liquid films and small droplets are formed, causing exhaustive interface between gas-liquid [2, 5, 6]. The mass transfer coefficient in the RPB was found to be 1-3 times that conventional packed beds [9, 10]. Owing to the high mass transfer coefficient and the plug flow pattern in the RPBs, reaching the steady-state take a little time in these reactors [11]. Currently, the RPBs have many applications in many chemical processes, e.g., absorption, desorption, distillation, synthesis of Nano-fibers of aluminum hydroxide, combined photolysis and catalytic ozonation of dimethyl phthalate [7, 12-17]. Owing to, flooding in the RPBs occur at high fluid flows rather than conventional packed beds, RPBs can be utilized at high gas flow rates [5, 18, 19]. On the other hands, Pressure drop in RPBs is higher than the conventional packed beds. Thus, the energy consumption is larger than the conventional packed beds [20-22]. By using centrifugal force can be increased interface

* Corresponding Author: A. R. Miroliaei (E-mail address: armiroliaei@uma.ac.ir)

Journal of Chemical and Petroleum Engineering, 2023, 57(2): 375- 389.
Publisher: University of Tehran, College of Engineering *DOI: 10.22059/jchpe.2023.354374.1422*
© Shamsedin Ghourejili, Ali Reza Miroliaei

areas between gas and liquid; the liquid is converted to spray in the RPBs like to spray dryer. Many researchers examined hydrodynamic parameters as experimental or simulation in the RPBs such as; Sung et al experimentally investigated the operating variables such as; gas flow rate, liquid flow rate, rotational speed of the pressure drop and mass-transfer. Their finding demonstrated that gas flow rate and rotational speed had a linear effect on the pressure drop and liquid flow rate had a little influence other one, on the pressure drop [5]. Keyvani et al considered the pressure drop in the RPB experimentally. They showed that dry-bed and wet-bed pressure drop were proportional to the square rotational speed as same as gas flow rate [23]. Lin et al considered the pressure drop and mass-transfer in the RPB experimentally. They understood, the RPB with blade packing's had lower pressure drop and larger mass transfer than the random and structure packings [24]. Yang et al investigated monophase flow in the RPB. They observed that inlet velocity influenced on the radial velocity and it was not influenced by the packing rotation. Also, rotational speed influenced on the tangential velocity and it was a key factor distribution fluid flow in the RPB [25]. Lierena et al surveyed the different feeding configuration of single-phase flow in the RPB. The obtained results demonstrated that gas injection placed on the top rotor, reduced gas tangential velocity. Their results showed that maldistribution of gas circling in the RPB [26]. Hamedi et al showed that three-dimensional steady state single phase flow in the RPB. The results revealed that tangential velocity vectors have the majority contribution in the velocity field of the packed bed section. Also, axial velocity vectors have the minor contribution to the velocity field in the housing section [27]. Martinez et al considered three-dimensional water-SO2 flow in the RPB. Theirs finding showed that rotational packing influenced the So2 flow distribution in the RPB. Also, it has not influenced on the water velocity field [28]. Shi et al examined the effect of rotational packing on the liquid flow in the RPB. They observed that at high rotational speeds, the liquid droplet diameter was dramatically smaller than the droplets at low rotating speeds. Furthermore, the addition static baffles between the layers of packing caused smaller liquid droplet. Therefore, the maldistribaution of liquid in the local area of packing could be diminished by increasing rotational speed [4]. Xie et al described the 2D CFD model of liquid flow in the RPB. The obtained results indicated that increasing rotational speed dramatically decreased liquid hold up and increased the degree of the liquid dispersion. Also, the liquid jet velocity slightly increased the liquid hold up [29]. YuGuo et al examined the liquid flow pattern such as film flow, droplet flow, pore flow within the reactors as a 2D and 3D. They revealed that the liquid maldistrubation could be countered by increasing rotating speed or the inlet velocity liquid. Also, the results revealed that liquid velocity strongly depended on the liquid inlet velocity [30]. Liu et al investigated liquid flow pattern in the outer cavity zone in the RPB with CFD and high-speed photography technology. The obtained results revealed that the liquid distribution in the outer cavity zone was chaotic. Also, liquid ligaments and droplets were not in every position of the packing outlet edge. The average droplet velocity in the outer cavity zone linearly increased with the increasing of the rotational speed, while liquid initial velocity did not influence the average velocity [31]. Lu et al illustrated the new model was based on the Kołodziej high porosity wire screen one-phase porous media model gas- liquid flow in the RPB. Unfortunately, there are no suitable porous media models that accurately describe the drag force between the gas and liquid, the gas and solids and the liquid and solids due to the high porosity and the stacked wire screen packing used in RPBs. So, the new model was presented. The new model was proposed for the Eulerian simulation of the gas-liquid two-phase flow in RPBs. They compared theirs new model with the current porous media models for traditional spherical or structured slit packed beds, according to the Attou, Lappalainen, Iliuta and Zhang models. Theirs finding revealed that the new model was very accurate for predicting the liquid flow in the RPB [32].

Lee et al modeled the RPB for the absorber and a stripper to carbon capture. They're fining was validated with published steady-state experimental data. The simulated result showed that minimizing the total energy of the MEA process [33].

Wang et al investigated the influence of micro-mixing efficiency during co-precipitation reaction in the RPB. The obtained result showed that the MOx-CeO2 (M = Cu, Co, Fe) catalysts prepared in the RPB reactor featured more M-O-Ce species. Also, 1.3 – 1.4 times concentration of oxygen vacancy more than those prepared in a stirred tank reactor [34].

Abolhasani et al investigated rotational speed, liquid flow rate and the volumetric ratio in the RPB reactor equipped with angled blade packings and high-frequency ultrasonic experimentally. The obtained results showed that the segregation index decreased as the rotational speed and liquid flow rate increased. Also, Blade packing with an angle of 45° has had the greatest effect on enhancing the micro mixing efficiency. Their findings demonstrated that the use of angled blade packing had a much greater effect of enhancing the micro mixing efficiency rather to the ultrasound [35].

Overall, many literatures investigated analysis single phase flow, the multi-phase flow velocity field and many hydrodynamic parameters such as pressure drop, liquid hold up in the RPB, and etc. So, scarce researchers examined the effect of nozzle numbers on the flow patterns. Therefore, the understanding of distribution liquid inlet in these types of reactors is scarce. In this paper, liquid inlet distribution in a 3D RPB with CFD is performed. The main object of this paper is to survey the effect 2 to 8 nozzles of water inlet on the behavior velocity field of air -water phase flow in the RPB with packing and with baffles.

CFD simulation

The Geometry of the RPB and Grid Refinement

Fig. 1 describes the sketch of the RPB. The RPB was consisted of two parts, rotor and housing which rotor is moved by a driving motor and housing is stationary. During the process; gas stream fed to the RPB from the stationary wall of the housing. Owing to the pressure gradient; the gas moved in the radial direction of the rotor. At the end, the gas would exhaust from the top of the RPB.

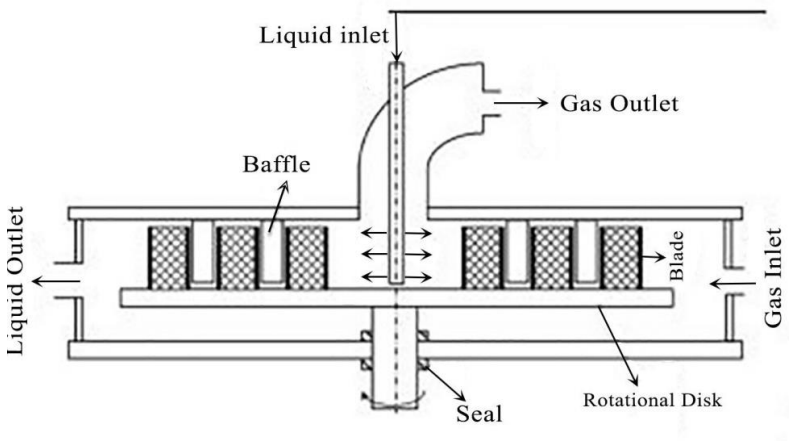

Fig. 1. Schematic of the RPB

The water flow rate was streamed to the rotor from the liquid distributor. Water flow sprayed by the liquid distributor. So, nozzles were mounted on it. The air and water streams contacted at the radial direction in the RPBs. The water streamed in the rotor by centrifugal force that was higher than the gravitational force. Water streams were collected at the static housing and eventually would be expelled from the bottom of the RPBs [1, 4, 5]. Two disks were set 2cm apart. The blade packing and baffles have been built from stainless steel mesh. The blade

packing was mounted on the bottom disk and the blade baffles were fixed on the top disk, respectively. In this paper, 40 blade packing, and 16 blade baffles were used for the analysis two- phase flows in the RPB. Three layers of the blade packing and two layers of the blade baffles were mounted on the RPB; 8, 16, 16 for the packing and 8, 8 for the blade baffles, respectively. The inner and outer radius of the rotor was 1.8, and 7.8 cm; respectively. The center distance between layers of the blade packing was set 1.2 cm. The blade packing has values with the radial width, and axial height of 1.2, and 1.8 cm; respectively. Also, the blade baffles have values with the radial width, and axial height of 0.6, and 1.5cm; respectively. The liquid distributor has 6 nozzles with diameter values of 0.50 mm for each nozzle. The porosity of any blade packing was used 0.99. In this work, RPB with blade packing is inspired RPB with packing. Also, RPB with blade packing that baffles fixed between layers of packing is inspired RPB with baffles [5]. Fig. 2 shows the three-dimensional structure and mesh structure of RPB with blade packing and baffles. Fig. 3 shows the schematic of nozzle numbers in the RPB. The simulation was performed with Ansys fluent16.0.

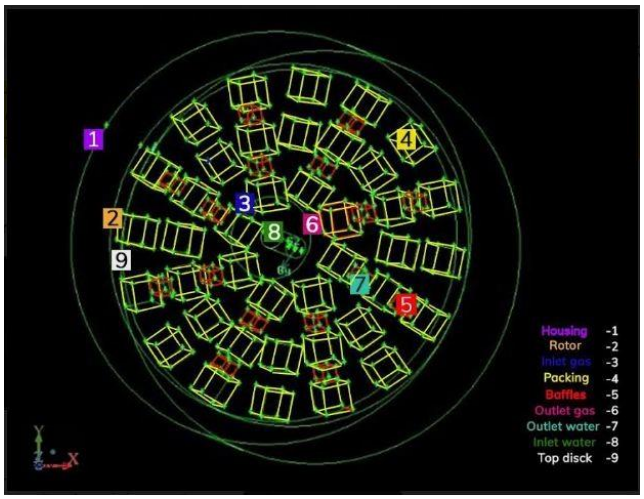

(a)

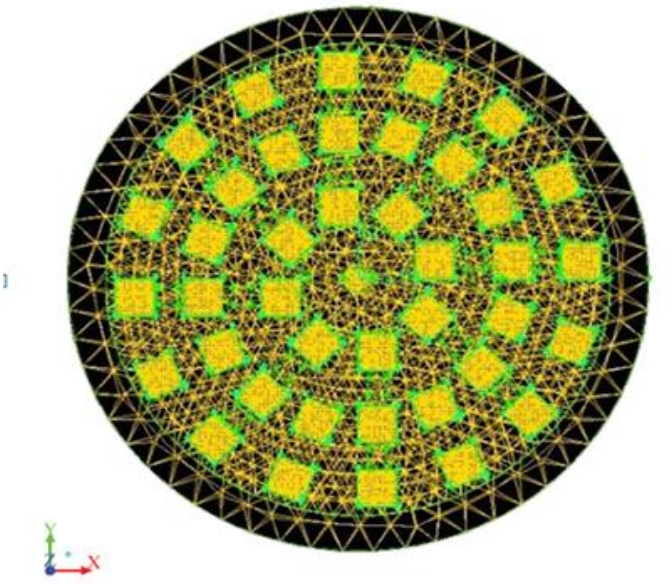

(b)

Fig. 2. 3D structure of the RPB with blade packing and baffles (a); 3D mesh structure of the RPB with blade packing and baffles from the top view (b)

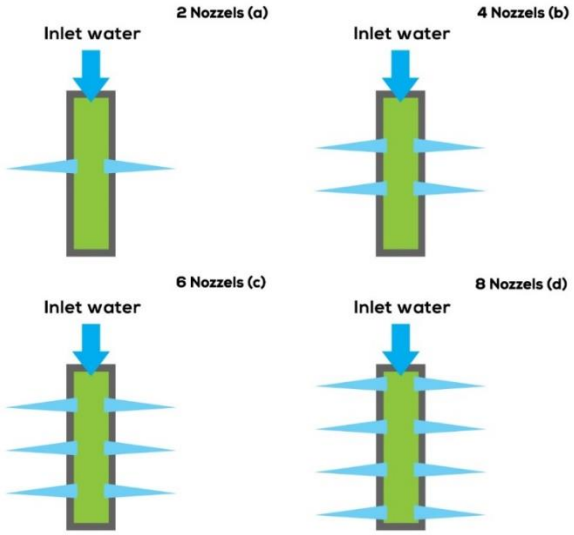

Fig. 3. Schematic of Nozzle numbers in the RPB; 2Nozzel numbers (a), 4Nozzel numbers (b), 6Nozzel numbers (c), 8 Nozzle numbers (d)

Mesh Independency

To simulate, the best mesh elements should be obtained. Then, mesh independence was investigated. Many types of mesh elements were examined. At the end, the RPB with packing, by 691113 mesh elements and node 704930 was used. Also, the RPB with baffles by 757025 mesh elements and node 718246 was used**.** To simulate, the best mesh elements should be attained. So, mesh independence is examined. To this, five mesh elements are investigated. RPB without baffles, mesh 1 with 148829 elements, mesh 2 with 167664 elements, mesh3 with 691113 elements, mesh 4 with 763336, and mesh 5 with 797552 elements was investigated. Also, RPB with baffle, mesh 1 with 638065 elements, mesh 2 with 757025 elements, mesh 3 with 780364 elements, mesh 4 with 736541 elements, and mesh 5 with 615384 elements are investigated; respectively. Owing to, the difference percent of pressure drop in the RPB without baffle between mesh 2, 3, 5 was lower than 0.07. So, mesh 3 with 691113 elements, was chosen. Also, the difference percent of pressure drop between mesh 2, 3, 4 in the RPB with baffle was lower than 0.12. So, mesh 2 with 757025 elements was chosen; respectively. Fig. 4 shows mesh independence in the RPB with and without baffle.

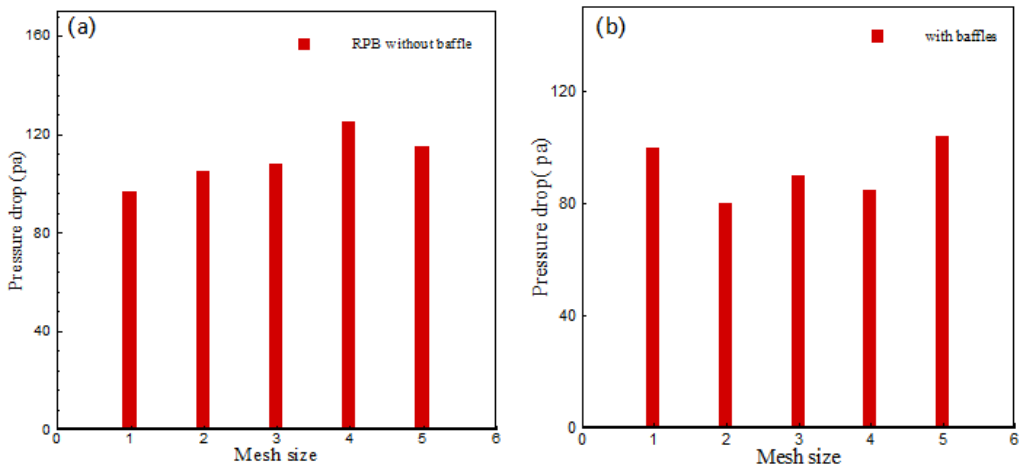

Fig.4. the mesh independence in the RPB; without baffle (a), and RPB with baffle (b)

Governing Equations

Simulation two-phase flows in the RPB was considered. Then, two kinds of momentum equation were solved. Due to, flows in the RPB have the high-speed rotating flows, flows involving porous media, the PRESTO Scheme was used. Also, an interpolation scheme with PRESTO technique was used. In this paper, the mixed model as a Eulerian-Eulerian method is used to simulate two-phase flows in a rotating packed bed. Also, the single reference frame (SRF) model was used. Owing to, flows rotation in the RPB; The realizable k-ε model was adopted. owing to, high Reynolds number of air and water flows in the present study, the flow for the system was considered turbulent. So, besides the continuum and momentum equations, turbulence equations were also considered. The continuity equation for the mixture is as follow.

$$\frac{\partial}{\partial t}\left(\rho_m\right)+\nabla.\left(\rho_m \overrightarrow{v_m}\right)=0 \tag{1}$$

where, $\overrightarrow{v_m}$, ρ_m are average velocity and average density mixture; respectively. These parameters obtained with Eqs. 2 and 3; respectively as follow. In these equations α_k is the volume fraction of phase k.

$$\overrightarrow{v_m}=\frac{\sum_{k=1}^{n}\alpha_k \rho_k \overrightarrow{v_k}}{\rho_m} \tag{2}$$

$$\rho_m=\sum_{k=1}^{n}\alpha_k \rho_k \tag{3}$$

Also, the momentum equation is obtained by Eq. 4. That n is a number of phases and $\vec{F}$ is volume force. Furthermore, the μ_m is viscosity mixture that obtained with in Eq. 5. c_k is the mass fraction of phase k that attained with Eq. 6. The release velocity and relative velocity are coupled by Eq. 7.

$$\frac{\partial}{\partial t}(\rho_m \overrightarrow{v_m})+\nabla.(\rho_m \overrightarrow{v_m}\overrightarrow{v_m})=\left[-\nabla.\mathrm{p}+\nabla.(\mu_m(\nabla\overrightarrow{v_m}+\overrightarrow{v_m}^{T})\right]+\rho_m\vec{g}+\vec{F}+\nabla.(\sum_{K=1}^{n}\alpha_k\rho_k\overrightarrow{v_{dr,k}}\overrightarrow{v_{dr,k}}) \tag{4}$$

$$\mu_m=\sum_{k=1}^{n}\alpha_k\mu_k \tag{5}$$

$$c_k=\frac{\alpha_k\rho_k}{\rho_m} \tag{6}$$

$$\overrightarrow{v_{dr,p}}=\overrightarrow{v_{pq}}-\sum_{k=1}^{n}c_k\overrightarrow{v_{qk}} \tag{7}$$

That relative velocity is obtained within Eq. 8. In this equation, τ_p is relax time of particle that obtained with Eq. 9. Also, acceleration is extracted with Eq. 10. The release speed is presented by Eq. 11. Volume fraction of Second phase p was present with Eq. 12.

$$\overrightarrow{v_{pq}}=\frac{\tau_p}{f_{drag}}\frac{(\rho_p-\rho_m)}{\rho_p}\vec{\alpha} \tag{8}$$

$$\tau_p = \frac{\rho_p d_p^2}{18\mu_q} \tag{9}$$

$$\vec{\alpha} = \vec{g} - (\overrightarrow{v_m}.\nabla)\overrightarrow{v_m} - \frac{\partial \overrightarrow{v_m}}{\partial t} \tag{10}$$

$$\overrightarrow{v_{pq}} = \frac{(\rho_p - \rho_m)d_p^2}{18\mu_q f_{drag}}\vec{\alpha} - \frac{v_m}{\alpha_p \sigma_D}\nabla_{\alpha q} \tag{11}$$

$$\frac{\partial}{\partial t}(\alpha_p \rho_p) + \nabla.(\alpha_p \rho_p \overrightarrow{v_m}) = -\nabla.(\alpha_p \rho_p \overrightarrow{v_{dr,p}}) + \sum_{q=1}^{n}(\dot{m}_{qp} - \dot{m}_{pq}) \tag{12}$$

Also, the transport equation for the turbulent kinetic energy, k and the dissipation rate, ε, in the realizable k-ε model is presented with Eq. 13, Eq. 14 as follow [36].

$$\frac{\partial(\rho k)}{\partial t} + \frac{\partial(\rho k u_j)}{\partial x_j} = \frac{\partial}{\partial x_j}\left[((\mu + \frac{\mu_t}{\sigma_k})\frac{\partial k}{\partial x_j})\right] + G_k + G_b - \rho\varepsilon \tag{13}$$

$$\frac{\partial(\rho\varepsilon)}{\partial t} + \frac{\partial(\rho\varepsilon u_j)}{\partial x_j} = \frac{\partial}{\partial x_j}\left[(\mu + \frac{\mu_t}{\sigma_\varepsilon})\frac{\partial \varepsilon}{\partial x_j}\right] + \rho C_1 S\varepsilon - \rho C_2 \frac{\varepsilon^2}{k + \sqrt{\nu\varepsilon}} \tag{14}$$

$$+C_{1\varepsilon}\frac{\varepsilon}{k}C_{3\varepsilon}G_b$$

where:

$$C_1 = \max\left[0.43, \frac{\eta}{\eta + S}\right]$$

$$\eta = S\frac{k}{\varepsilon}$$

$$S = \sqrt{2S_{ij}S_{ij}}$$

Also, σ_k and σ_ε are Prandtl numbers. G_k and G_b generation of turbulent kinetic energy. In the simulation, the air was considered as a continuous phase, and water as a dispersed phase. The finite volume discretized equations were solved. Coupled algorithm was used for velocity-pressure coupling, and second-order upwind scheme discretization method were employed to increase the precise of the results. In this work, the RPB operated in the range of rotational speed at 600-1000 rpm, inlet air flow rate of 10-40 lit/min, inlet water flow rate of 0.1-0.4 lit/min, and the pressure at the outlet was fixed atmospheric [37].

Results and Discussion

The Effect of Air Flow Rate on the Pressure Drop in the RPB with Packing and Baffles

Figs. 5a and 5b showed that the effect of air flow rate of the pressure drops in the constant water flow rate and rotational speed in the RPB with 6 nozzles. These figures demonstrated that at the constant water flow rate and rotational speed values; increasing the air flow rate increased the pressure drop. To validate the results, simulation data were compared with the experimental

data of Sung et al. The obtained results satisfied with the experimental data with deviations generally within 14%.

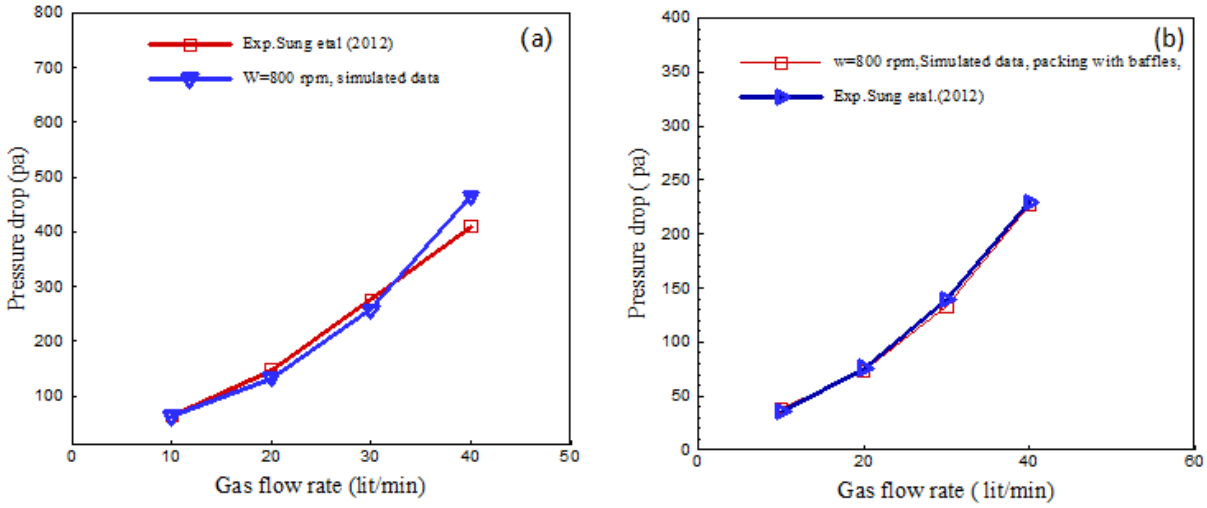

Fig. 5. the effect of air flow rate on the wet- pressure drop in the RPB with 6 nozzles via blade packing (a); RPB via blade packing and baffles (b) at $Q_L = 0.30\ \frac{lit}{min}$,$\omega = 800$ rpm

The Effect of Nozzle Numbers on the Velocity Vector of Air

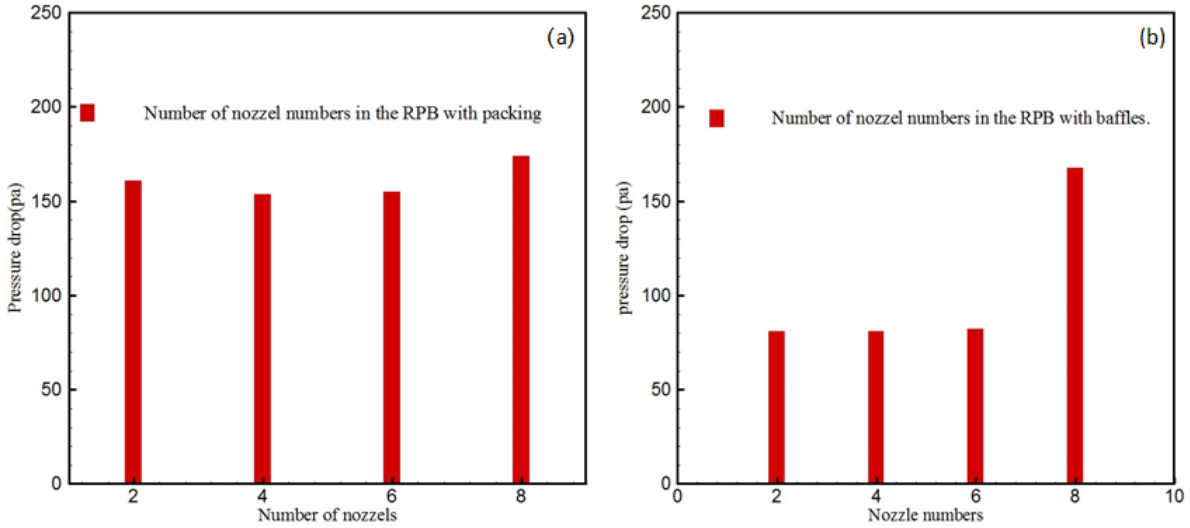

Fig. 6. the effect of nozzle on the wet- pressure drop in the RPB with 6 nozzles via blade packing (a); RPB with blade packing and baffles (b) at $Q_L = 0.30\ \frac{lit}{min}$, $Q_G = 20\ \frac{lit}{min}$ and 800 rpm

Figs. 6a and 6b depicted the effect of nozzles on the pressure drop in the constant water flow rate, air flow rate and rotational speed at $Q_L = 0.30\ \frac{\text{lit}}{\text{min}}$, $Q_G = 20\ \frac{\text{lit}}{\text{min}}$ and 800 rpm in the RPB, respectively. These figures demonstrated that, with increasing nozzle increased pressure drop.

Fig. 7 shows the airflow pattern at different nozzles in the RPB with packing. According to Figs. 6a to 6d, when the rotational speed, water and air flow rates were constant, RPB with 6 nozzles lead the velocity vectors of the air flow increased. Then, the momentum of the air flow incremented. One probably is slipping velocity between the air and water phases increased. Furthermore, RPB with 8 nozzles caused the air flow awayed from the uniform pattern. The

obtained results satisfied with the experimental data. These figures also demonstrated that the velocity field in the outer edge of the rotor was larger than the inner edge of rotor and housing.

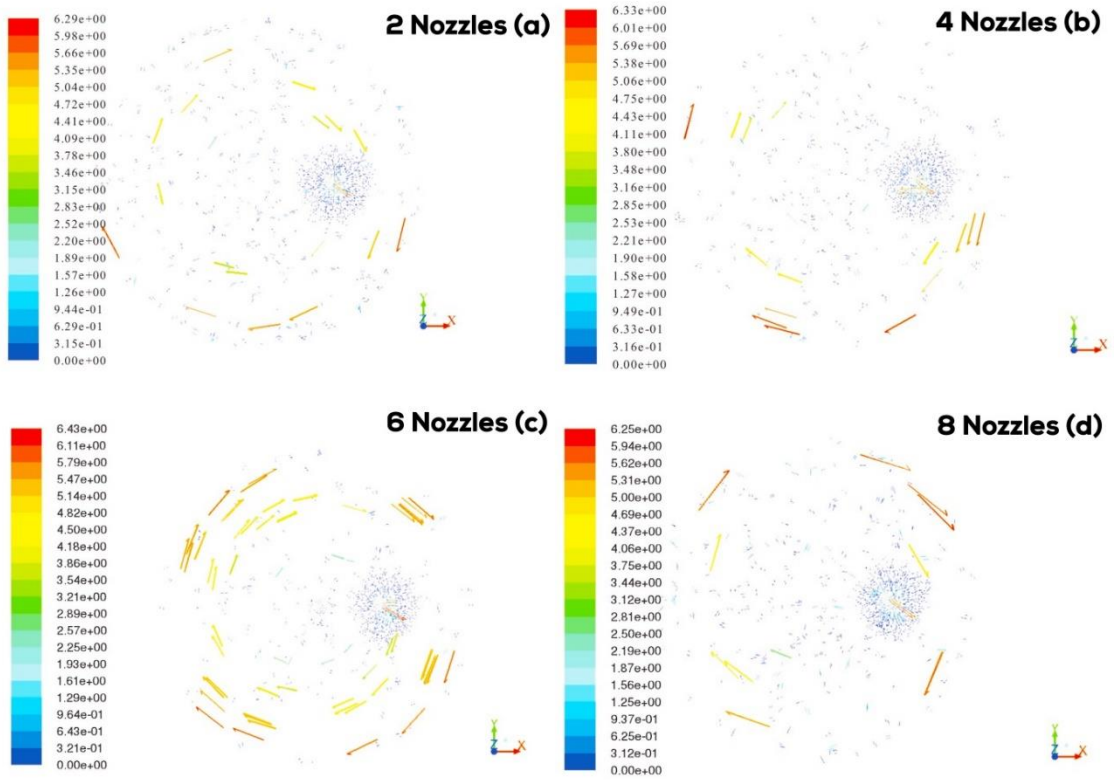

Fig. 7. The influence of nozzles on the air velocity vectors (m. s^{-1}) in the RPB with packing from the top view

Fig. 8 describes the flow pattern of the air in the RPB with baffles at different nozzles. As can be seen from Fig. 8, Increasing numbers of nozzle 2 to 6 caused the air velocity field incremented. According to Fig. 7 and Fig. 8, RPB with 6 nozzles at the constant rotational speed, air flow and water flow rates unlike the RPB with packing under similar operating condition; the air velocity vectors approached more uniform pattern pattern quickly. Furthermore, the presence of baffles in the RPB increased the drag force of baffles like to the packing on the water film. Thus, it leads to increase the air and water slip velocity [5]. Therefore, the baffles increased the momentum and velocity vectors of air flow. Also, the results showed that the RPB with 8 nozzles, air velocity field diminished. One probably is the water flow bulked the RPB. So, pressure drop increased. Therefore, flooding phenomena occurred in the RPB. As can be seen in Figs. 6a to 6d, the maximum air velocity vectors were at the rotor output.

The Effect of Nozzle Numbers on the Velocity Vector of Water Flow

Fig. 9 displays the effect of nozzles on the water velocity in the RPB with packing. According to Figs. 9a to 9d, at the rotational speed, water and air flow rates were constant, the velocity vectors of the water flow of RPB with 6, 8 can contribute to uniform rather than the RPB with 2, 4 nozzles all the rotor and housing. Therefore, increasing numbers of nozzles caused suitable distribution flow water.

Fig. 9 demonstrates the behavior of water flow at different nozzles in the RPB with baffles. According to Figs. 9a to 9d, at the rotational speed, water and air flow rates were constant, increasing nozzles 2 to 6, increased water velocity vectors in the RPB. Also, these figures showed that increasing nozzles 2 to 6, increased more water velocity gradient in the rotor. Furthermore, the water flow bulked in a total space of packing and housing in the RPB with 8 nozzles. So, the RPB reached to flooding. These figures also demonstrated that the velocity

field in the outer edge of the rotor was larger than the inner edge of the rotor. The obtained results good agreement with the experimental data.

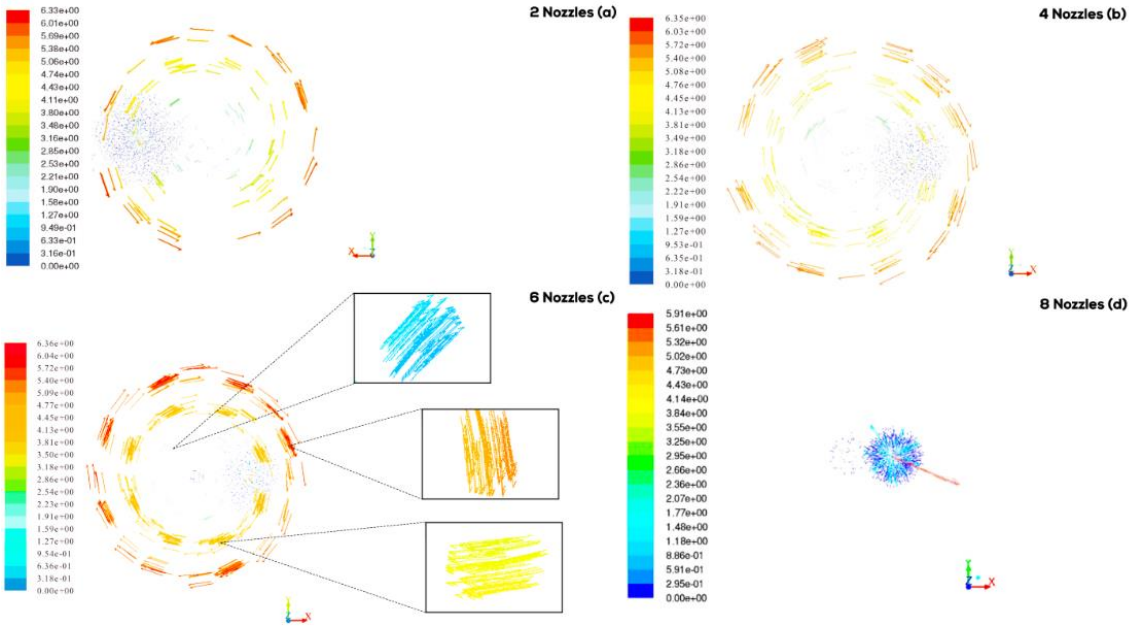

Fig. 8. The influence of nozzles on the air velocity vectors (m. s^{-1}) in the RPB with baffles from the top view

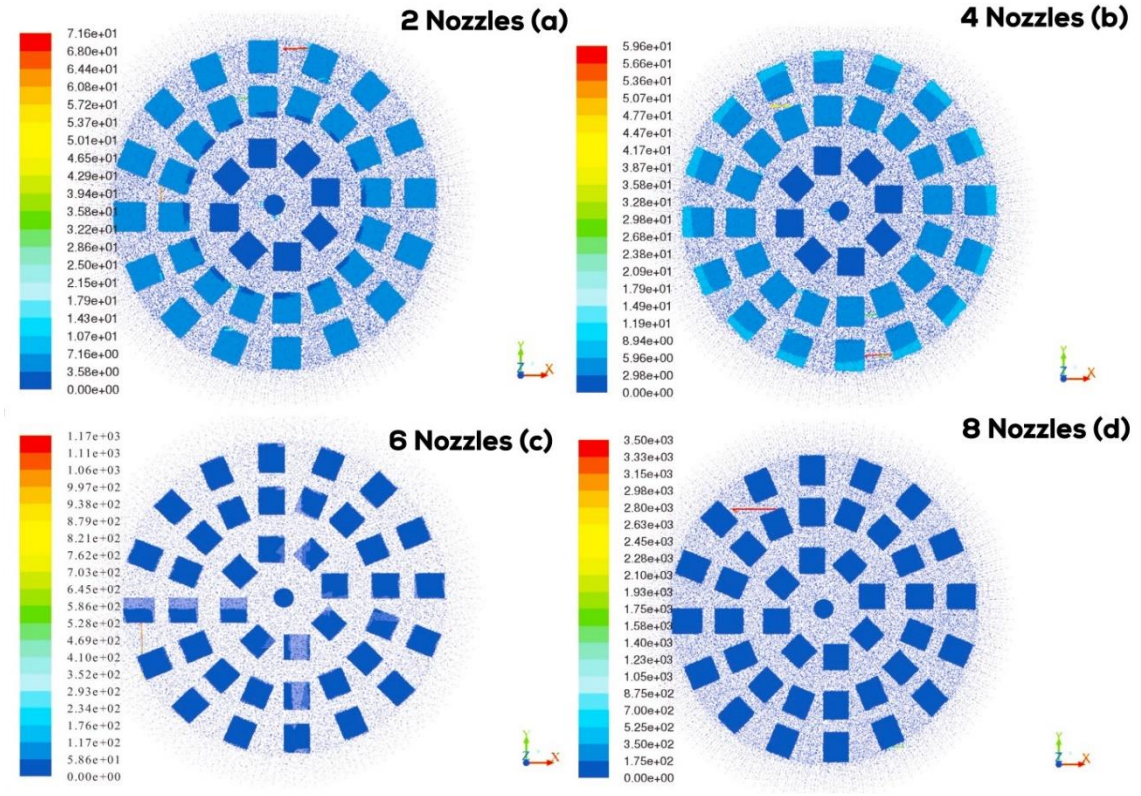

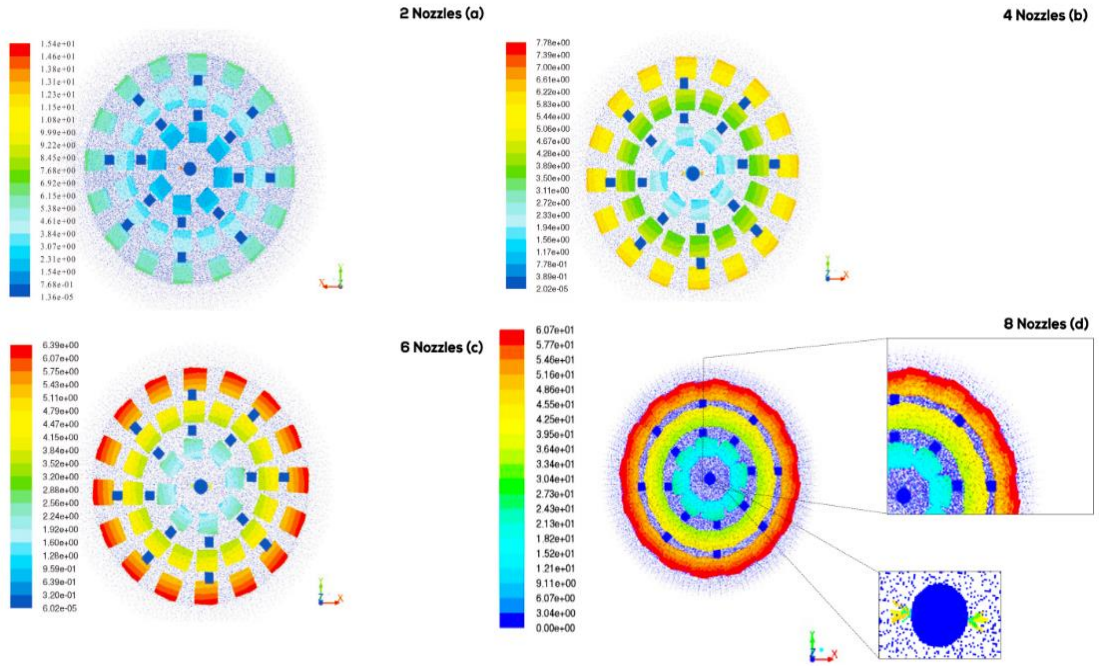

Fig. 9. The influence of nozzle numbers on the velocity vectors of water (m. s^{-1}) in the RPB with packing from the top view

Conclusion

RPBs have been recently used in the many chemical processes such as absorption, desorption, distillation, and etc. Owing to the high gravity field, RPBs can improve the exhaustive interface between air-water. In this paper, air-water analysis was conducted by using CFD. Thus, flow analysis in the RPB with packing and baffles was performed. First, the RPB with packing results demonstrated that increasing nozzle 2 to 6 increased velocity field of air flow. Also, RPB with 8 nozzles caused the air flow awayed from the uniform flow pattern. Second, the RPB with baffles, increasing nozzles from2 to 6 caused the air velocity field incremented. Also, the RPB with 8 nozzles, the air velocity field diminished. Furthermore, velocity vectors of water flow in the RPB with packing, increasing nozzles from2 to 8 were uniform distribution in all section of rotor and housing. Also, RPB with baffles, increasing nozzles from 2 to 6 can create gradient velocity vectors of water in all sections of the rotor and housing. Then, momentum of water flow increased. The obtained results were compared with the experimental data extracted from the RPB with 6 nozzles.

Furthermore, flooding phenomena occurred in the RPB with baffles with 8 nozzles. Under the same operating conditions, RPB with baffllles can improve the momentum flow of air and water. In the results demonstrated that RPB with packing and baffles with 6 nozzles, air flow has more momentum and reached the uniform flow pattern than the other nozzles.

Nomenclature

Prandel dispersion	σ_D
Turbulence dissipation rate ($m^2. s^{-3}$)	ε
Surface tension (kg. s^{-2})	σ_k
Acceleration (m. s^{-2})	α
Turbulence viscosity (pa.s)	μ_t
Particle density (kg. m^{-3})	ρ_p
Effective density (kg. m^{-3})	ρ_m

Effective viscosity(pa.s)	μ_m
Viscosity of phase k(pa.s)	μ_k
Rotational speed(rad.min^{-1})	ω
Volume fraction of phase k	α_k
Volume force	$\vec{F}$
produced viscosity	G
Diameter particle (m)	dp
Turbulence velocity mixture	v_m
Mass fraction of phase k	c_k
Mass flow rate of phase q to p (kg.s^{-1})	m_{qp}
Mass flow rate of phase p to q (kg.s^{-1})	m_{pq}
Momentum Source of phase k (rad.min^{-1}.m^{-3})	S_k
Average velocity of phase k (m. s^{-1})	$\overrightarrow{v_k}$
Average velocity mixture (m. s^{-1})	$\overrightarrow{v_m}$
Air flow rate (lit. min^{-1})	Q_G
water flow rate (lit. min^{-1})	Q_L

References

[1] Lin CC, Chen BC. Carbon dioxide absorption in a cross-flow rotating packed bed. Chemical engineering research and design. 2011 Sep 1;89(9):1722-9. https://doi.org/10.1016/j.cherd.2010.11.015.

[2] Lin CC, Wei TY, Hsu SK, Liu WT. Performance of a pilot-scale cross-flow rotating packed bed in removing VOCs from waste gas streams. Separation and purification technology. 2006 Dec 1;52(2):274-9. https://doi.org/10.1016/j.seppur.2006.05.003.

[3] Ouyang Y, Wang S, Xiang Y, Zhao Z, Wang J, Shao L. CFD analyses of liquid flow characteristics in a rotor-stator reactor. Chemical Engineering Research and Design. 2018 Jun 1; 134:186-97. https://doi.org/10.1016/j.cherd.2018.04.006.

[4] Shi X, Xiang Y, Wen LX, Chen JF. CFD analysis of liquid phase flow in a rotating packed bed reactor. Chemical Engineering Journal. 2013 Jul 15; 228:1040-9. https://doi.org/10.1016/j.cej.2013.05.081.

[5] Sung WD, Chen YS. Characteristics of a rotating packed bed equipped with blade packings and baffles. Separation and purification technology. 2012 Jun 1; 93:52-8. https://doi.org/10.1016/j.seppur.2012.03.033.

[6] Tan CS, Chen JE. Absorption of carbon dioxide with piperazine and its mixtures in a rotating packed bed. Separation and purification technology. 2006 Apr 15;49(2):174-80. https://doi.org/10.1016/j.seppur.2005.10.001.

[7] Xiuping L, Youzhi L, Zhiqiang L, Xiaoli WA. Continuous distillation experiment with rotating packed bed. Chinese journal of chemical engineering. 2008 Jan 1;16(4):656-62. https://doi.org/10.1016/S1004-9541(08)60137-8.

[8] Ramshaw C, Mallinson RH, inventors; Imperial Chemical Industries Ltd, assignee. Mass transfer process. United States patent US 4,283,255. 1981 Aug 11.

[9] Chen YS, Lin FY, Lin CC, Tai CY, Liu HS. Packing characteristics for mass transfer in a rotating packed bed. Industrial & engineering chemistry research. 2006 Sep 27;45(20):6846-53. https://doi.org/10.1021/ie060399l.

[10] Zhao H, Shao L, Chen JF. High-gravity process intensification technology and application. Chemical Engineering Journal. 2010 Feb 1;156(3):588-93. https://doi.org/10.1016/j.cej.2009.04.053.

[11] Chiu CY, Chen YH, Huang YH. Removal of naphthalene in Brij 30-containing solution by ozonation using rotating packed bed. Journal of hazardous materials. 2007 Aug 25;147(3):732-7. https://doi.org/10.1016/j.jhazmat.2007.01.068.

[12] Chang CC, Chiu CY, Chang CY, Chang CF, Chen YH, Ji DR, Yu YH, Chiang PC. Combined photolysis and catalytic ozonation of dimethyl phthalate in a high-gravity rotating packed bed. Journal of Hazardous Materials. 2009 Jan 15;161(1):287-93. https://doi.org/10.1016/j.jhazmat.2008.03.085.

[13] Chen JF, Shao L, Guo F, Wang XM. Synthesis of nano-fibers of aluminum hydroxide in novel rotating packed bed reactor. Chemical Engineering Science. 2003 Feb 1;58(3-6):569-75. https://doi.org/10.1016/S0009-2509(02)00581-X.

[14] Jassim MS, Rochelle G, Eimer D, Ramshaw C. Carbon dioxide absorption and desorption in aqueous monoethanolamine solutions in a rotating packed bed. Industrial & engineering chemistry research. 2007 Apr 25;46(9):2823-33. https://doi.org/10.1021/ie051104r.

[15] Mondal A, Pramanik A, Bhowal A, Datta S. Distillation studies in rotating packed bed with split packing. Chemical Engineering Research and Design. 2012 Apr 1;90(4):453-7. https://doi.org/10.1016/j.cherd.2011.08.008.

[16] Qian Z, Xu LB, Li ZH, Li H, Guo K. Selective absorption of H2S from a gas mixture with CO2 by aqueous N-methyldiethanolamine in a rotating packed bed. Industrial & engineering chemistry research. 2010 Jul 7;49(13):6196-203. https://doi.org/10.1021/ie100678c.

[17] Wang W, Zou HK, Chu GW, Weng Z, Chen JF. Bromination of butyl rubber in rotating packed bed reactor. Chemical engineering journal. 2014 Mar 15; 240:503-8. https://doi.org/10.1016/j.cej.2013.10.095.

[18] Lockett MJ. Flooding of rotating structured packing and its application to conventional packed-columns. Chemical engineering research & design. 1995;73(4):379-84.

[19] Lin CC, Chen BC, Chen YS, Hsu SK. Feasibility of a cross-flow rotating packed bed in removing carbon dioxide from gaseous streams. Separation and purification technology. 2008 Sep 22;62(3):507-12. https://doi.org/10.1016/j.seppur.2008.02.019.

[20] Zheng C, Guo K, Feng Y, Yang C, Gardner NC. Pressure drops of centripetal gas flow through rotating beds. Industrial & engineering chemistry research. 2000 Mar 6;39(3):829-34. https://doi.org/10.1021/ie980703d

[21] Ratheesh S, Kannan A. Holdup and pressure drop studies in structured packings with catalysts. Chemical Engineering Journal. 2004 Nov 15;104(1-3):45-54. https://doi.org/10.1016/j.cej.2004.08.004.

[22] Said W, Nemer M, Clodic D. Modeling of dry pressure drop for fully developed gas flow in structured packing using CFD simulations. Chemical Engineering Science. 2011 May 15;66(10):2107-17. https://doi.org/10.1016/j.ces.2011.02.011.

[23] Keyvani M. Operating characteristics of rotating beds. Case Western Reserve University; 1989.

[24] Lin CC, Jian GS. Characteristics of a rotating packed bed equipped with blade packings. Separation and purification technology. 2007 Mar 15;54(1):51-60. https://doi.org/10.1016/j.seppur.2006.08.006.

[25] Yang W, Wang Y, Chen J, Fei W. Computational fluid dynamic simulation of fluid flow in a rotating packed bed. Chemical engineering journal. 2010 Feb 1;156(3):582-7. https://doi.org/10.1016/j.cej.2009.04.013.

[26] Llerena-Chavez H, Larachi F. Analysis of flow in rotating packed beds via CFD simulations—Dry pressure drop and gas flow maldistribution. Chemical Engineering Science. 2009 May 1;64(9):2113-26. https://doi.org/10.1016/j.ces.2009.01.019.

[27] Hamedi M, Haghshenas MF, Esfahany MN. Computational fluid dynamics analysis of fluid flow in a novel rotating packed bed. In13th Iranian National Chemical Engineering Congress & 1st International Regional Chemical and Petroleum Engineering 2010 Oct (pp. 25-28).

[28] Martínez EL, Jaimes R, Gomez JL, Maciel Filho R. CFD simulation of three-dimensional multiphase flow in a rotating packed bed. InComputer Aided Chemical Engineering 2012 Jan 1 (Vol. 30, pp. 1158-1162). Elsevier. https://doi.org/10.1016/B978-0-444-59520-1.50090-7.

[29] Xie P, Lu X, Yang X, Ingham D, Ma L, Pourkashanian M. Characteristics of liquid flow in a rotating packed bed for CO2 capture: A CFD analysis. Chemical Engineering Science. 2017 Nov 23; 172:216-29. https://doi.org/10.1016/j.ces.2017.06.040.

[30] Guo TY, Cheng KP, Wen LX, Andersson R, Chen JF. Three-dimensional simulation on liquid flow in a rotating packed bed reactor. Industrial & Engineering Chemistry Research. 2017 Jul 19;56(28):8169-79. https://doi.org/10.1021/acs.iecr.7b01759.

[31] Liu Y, Wu W, Luo Y, Chu GW, Liu W, Sun BC, Chen JF. CFD simulation and high-speed photography of liquid flow in the outer cavity zone of a rotating packed bed reactor. Industrial & Engineering Chemistry Research. 2019 Mar 8;58(13):5280-90. https://doi.org/10.1021/acs.iecr.8b05718.

[32] Lu X, Xie P, Ingham DB, Ma L, Pourkashanian M. A porous media model for CFD simulations of gas-liquid two-phase flow in rotating packed beds. Chemical Engineering Science. 2018 Nov 2; 189:123-34. https://doi.org/10.1016/j.ces.2018.04.074.

[33] Im D, Jung H, Lee JH. Modeling, simulation and optimization of the rotating packed bed (RPB) absorber and stripper for MEA-based carbon capture. Computers & Chemical Engineering. 2020 Dec 5; 143:107102. https://doi.org/10.1016/j.compchemeng.2020.107102.

[34] Wang BJ, Chu GW, Li YB, Duan XZ, Wang JX, Luo Y. Intensified micro-mixing effects on evolution of oxygen vacancies of CeO2-based catalysts for improved CO oxidation. Chemical Engineering Science. 2021 Nov 23; 244:116814. https://doi.org/10.1016/j.ces.2021.116814.

[35] Jamaat SS, Abolhasani M. Effect of blade packing structure and high-frequency ultrasound on micromixing efficiency enhancement in an RPB reactor. Chemical Engineering Research and Design. 2022 Dec 1; 188:197-208. https://doi.org/10.1016/j.cherd.2022.09.048.

[36] Guo TY, Cheng KP, Wen LX, Andersson R, Chen JF. Three-dimensional simulation on liquid flow in a rotating packed bed reactor. Industrial & Engineering Chemistry Research. 2017 Jul 19;56(28):8169-79. https://doi.org/10.1021/acs.iecr.7b01759.

[37] ANSYS FLUENT 12.0.16. Theory Guide. ANSYS Inc., 2009.

How to cite: Ghourejili S, Miroliaei AR. Influence of Nozzle Numbers on Analysis of Air-Water Flow in a Rotating Packed Bed with Computational Fluid Dynamics. Journal of Chemical and Petroleum Engineering. 2023; 57(2): 375-389.